

Bessel-Gauss pulses

P. L. Overfelt

Physics Division, Research Department, Naval Weapons Center, China Lake, California 93555-6001

(Received 29 October 1990; revised manuscript received 29 April 1991)

A family of exact pulse solutions of the homogenous free-space scalar wave equation is obtained. These solutions describe moving modified Bessel-Gauss pulses. They include the fundamental Gaussian pulse and the Bessel beam solutions as special cases. The zeroth-order Bessel-Gauss pulse is shown to be more highly localized than the fundamental Gaussian solution because of its extra spectral degree of freedom. A superposition of Bessel-Gauss pulses is used to create a splash pulse that is more localized than the Ziolkowski splash pulse.

I. INTRODUCTION

In recent years, a number of exact solutions of the three-dimensional scalar wave equation have been discovered that describe localized transmission of electromagnetic energy in space-time [1-9]. One of these solutions, the moving modified Gaussian pulse [2], was shown to maintain its Gaussian profile during propagation with only local variations. Another solution, the Bessel beam [6,7], has been shown, via both experiment and numerical simulation, to exhibit diffraction-free propagation over a limited range.

In accord with the above, we have derived a family of exact solutions to the scalar wave equation that contain both of the above solutions as special cases when appropriate limits are taken. Specifically for the homogeneous free-space scalar wave equation,

$$(\Delta - \partial_{ct}^2)\Phi_n(\mathbf{r}, t) = 0, \tag{1}$$

we have found that (1) is satisfied by

$$\Phi_n(\mathbf{r}, t) = \frac{a_1}{V} J_n \left[\frac{\kappa a_1 \rho}{V} \right] \exp \left[\pm i n \phi - \frac{\beta \rho^2}{V} - \frac{i \kappa^2 a_1 \xi}{4 \beta V} + i \beta \eta \right], \tag{2}$$

where $\xi = z - ct$ and $\eta = z + ct$ are the transformed coordinates, $V = a_1 + i \xi$ is the complex variance, ρ and ϕ are the usual transverse cylindrical coordinates, a_1 is a beam-source location term, and κ and β are spectral parameters governed by the constraint equation

$$\kappa^2 = 4 \alpha \beta, \tag{3}$$

as indicated by the bidirectional traveling-plane-wave representation [9]. Thus the zeroth-order symmetric solution,

$$\Phi_0(\mathbf{r}, t) = \frac{a_1}{V} J_0 \left[\frac{\kappa a_1 \rho}{V} \right] \exp \left[-\beta \left[\frac{\rho^2}{V} - i \eta \right] - \frac{i \kappa^2 a_1 \xi}{4 \beta V} \right], \tag{4}$$

can be described as a modulated moving Bessel-Gauss pulse. Equation (4) is derived in Appendix A. We show an alternative derivation using a bidirectional plane-wave decomposition in Appendix B.

II. BESSEL-GAUSS PULSE BEHAVIOR

Taking the limit of (4) as κ approaches zero, we have

$$\psi_G(\mathbf{r}, t) = \lim_{\kappa \rightarrow 0} \Phi_0(\mathbf{r}, t) = \frac{a_1}{V} e^{-\beta(\rho^2/V - i\eta)}, \tag{5}$$

which is Ziolkowski's fundamental Gaussian pulse [2,8].

By allowing a_1 to approach infinity, and using the beam spread, $A = a_1 + (\xi^2/a_1)$, and the phase front curvature, $R = \xi + (a_1^2/\xi)$, to obtain

$$\lim_{a_1 \rightarrow \infty} \left[\frac{a_1}{V} \right] = \lim_{a_1 \rightarrow \infty} \left[\frac{a_1}{A} - \frac{ia_1}{R} \right] = 1, \tag{6}$$

we find that

$$\psi_B(\mathbf{r}, t) = \lim_{a_1 \rightarrow \infty} \Phi_0(\mathbf{r}, t) = J_0(\kappa \rho) e^{-i \alpha \xi} e^{i \beta \eta}, \tag{7}$$

which is Durnin's Bessel beam solution in bidirectional traveling-plane-wave form with $\alpha = \kappa^2/4\beta$.

We would like to compare the propagation characteristics of the fundamental Gaussian and zeroth-order Bessel-Gauss pulses. For $\rho = 0, z = ct$ ($\xi = 0$),

$$\text{Re}[\psi_G(\mathbf{r}, t)] = \text{Re}[\Phi_0(\mathbf{r}, t)] = \cos 2\beta z, \tag{8}$$

indicating that both pulses' initial amplitudes are recovered periodically and thus they have the same type of time history behavior [8].

For a given time, Fig. 1 is a three-dimensional plot of the fundamental Gaussian pulse, $[\text{Re}(\psi_G)]^2$, for $a_1 = 1$ cm, $t = 0, \beta = 0.3333 \text{ cm}^{-1}, \kappa = 0$. Figure 2 shows a plot of the Bessel-Gauss pulse for the same values of the above parameters but with $\kappa = 3 \text{ cm}^{-1}$, giving a ratio of $\kappa/\beta = 9$. The Bessel-Gauss pulse is more localized about the transverse axis ($z = 0$) and also about the propagation axis when compared with the fundamental Gaussian. In general, we find that for $\kappa/\beta < 1$, the Bessel-Gauss pulse is very similar to the fundamental Gaussian and exhibits a plane-wave character for small β values and a particlelike

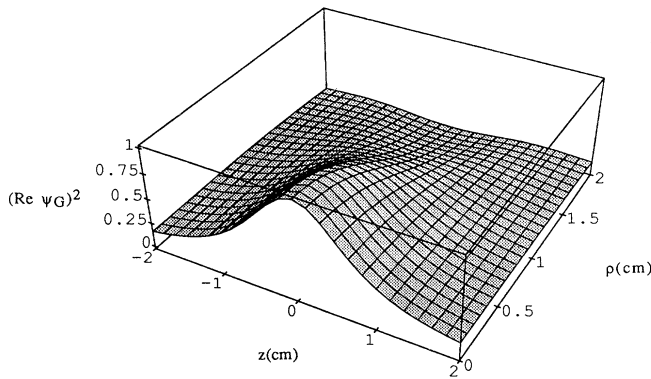


FIG. 1. Fundamental Gaussian pulse with $a_1=1$ cm, $t=0$, $\beta=0.3333$ cm $^{-1}$, $\kappa=0$ cm $^{-1}$.

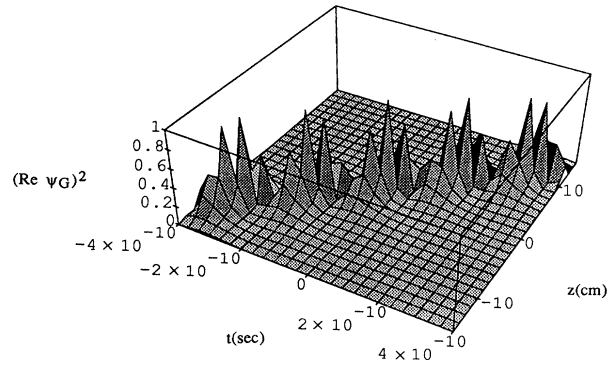


FIG. 3. Fundamental Gaussian pulse with $a_1=1$ cm, $\rho=0$, $\beta=0.3333$ cm $^{-1}$, $\kappa=0$ cm $^{-1}$.

character for larger β values. For $\kappa/\beta > 1$, it exhibits a particlelike character and is highly localized near both the transverse and propagation axes as κ increases. Because of its extra spectral degree of freedom, for any given value of β (by simply increasing κ), one can obtain a Bessel-Gauss pulse that is more localized in space than the fundamental Gaussian.

Figure 3 shows a three-dimensional plot of the fundamental Gaussian for a given value of the transverse coordinate, i.e., $\rho=0$, and shows $\{\text{Re}[\psi_G(\mathbf{r},t)]\}^2$ versus the propagation distance z and the time for $\beta=0.3333$ cm $^{-1}$ $a_1=1$ cm. We see that the pulse moves along a straight line in the z - t plane with changing amplitude. The pulse centers at $z=ct$ with $z=n\pi/\beta$ are not clearly defined. Figure 4 shows the same plot of a Bessel-Gauss pulse, $\kappa/\beta=9$, with the same parameters as in Fig. 3. Figure 4 shows the complete separation of each pulse center and shows that this Bessel-Gauss pulse is highly localized in time as well as space.

The Bessel-Gauss family of solutions to the three-dimensional scalar wave equation is another example of solutions obeying the general ansatz

$$\Phi_n(\mathbf{r},t) = G_n(\rho,\phi,\xi)e^{i\beta\eta}, \tag{9}$$

where

$$G_n(\rho,\phi,\xi) = \frac{a_1}{V} J_n \left[\frac{\kappa a_1 \rho}{V} \right] \exp \left[-\frac{\beta \rho^2}{V} - \frac{i\kappa^2 a_1 \xi}{4\beta V} \pm in\phi \right] \tag{10}$$

is a function of ρ , ϕ , and $(z-ct)$ only. The G_n are exact solutions to a free-particle Schrödinger equation having the form

$$\nabla_t^2 G_n + 4i\beta \frac{\partial G_n}{\partial \xi} = 0. \tag{11}$$

Considering the ansatz in (9), the Bessel-Gauss pulse is composed of a general wave traveling at a velocity c along the $+z$ -axis and a plane wave of wave number β traveling along the $-z$ axis at a velocity c [3,4]. A comparison of the function G_0 in (10) with the zeroth-order Bessel-Gauss solution in (4) is shown in Figs. 5–9. Assuming that $t=0$ and choosing the maximum transverse value of each function that occurs at $\rho=0$, these figures compare $[\text{Re}(G_0)]^2$ and $[\text{Re}(\Phi_0)]^2$ for various values of β , κ , and a_1 . In each instance, G_0 is the envelope of the entire solution to the wave equation. For $\kappa/\beta \leq 1$, G_0 envelopes completely the maximum of Φ_0 , but does not in-

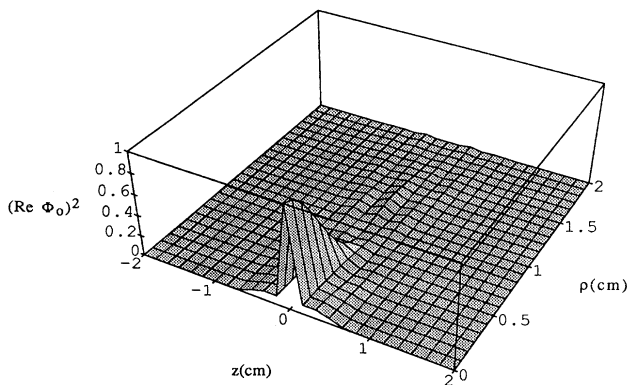


FIG. 2. Bessel-Gauss pulse with $a_1=1$ cm, $t=0$, $\beta=0.3333$ cm $^{-1}$, $\kappa=3$ cm $^{-1}$.

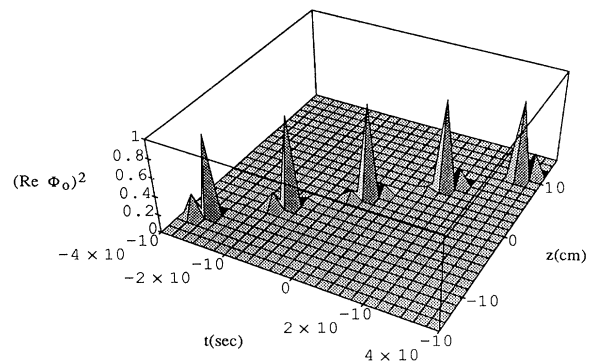
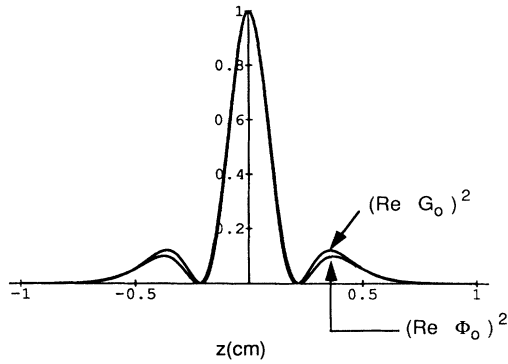


FIG. 4. Bessel-Gauss pulse with $a_1=1$ cm, $\rho=0$, $\beta=0.3333$ cm $^{-1}$, $\kappa=3$ cm $^{-1}$.



$$(\rho = 0, t = 0, a_1 = 1, \beta = 0.3333, \kappa = 3)$$

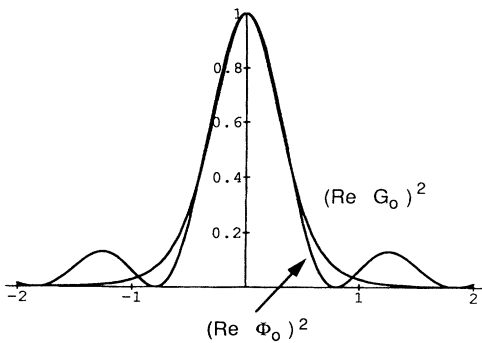
FIG. 5. Comparison of Bessel-Gauss solution Φ_0 , and its envelope G_0 with $\rho=0, t=0, a_1=1 \text{ cm}, \beta=0.3333 \text{ cm}^{-1}, \kappa=3 \text{ cm}^{-1}$.

clude the sidelobes very well. For $\kappa/\beta > 1$, G_0 almost completely encloses Φ_0 for values of $a_1=1$. If a_1 is decreased, not only is Φ_0 completely enclosed by G_0 , but the sharpness of its maximum and the damping of its sidelobes is very clear.

Figure 10 shows a time history of the G_0 function and plots the $[\text{Re}(G_0)]^2$ as a function of z for different times. Figure 11 shows the same plot for Φ_0 . The envelope G_0 , since it is a function of $(z - ct)$ and not of $(z + ct)$, travels without deforming in the $+z$ direction at velocity c . The complete Bessel-Gauss pulse also travels in the $+z$ direction but it deforms as t is increased from zero, losing amplitude and its symmetry, but reforming to its $t=0$ shape and maximum amplitude when

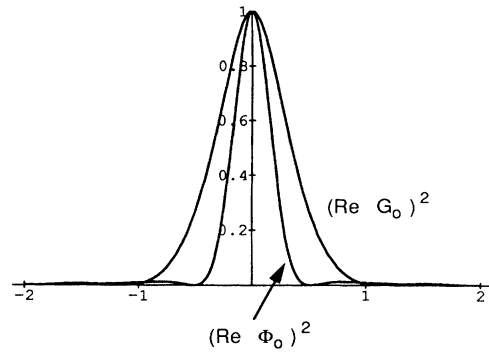
$$|\cos 2\beta z| = |\cos 2\beta ct| = 1. \quad (12)$$

Thus for appropriate values of z, t , and β , the pulse Φ_0 reforms to its initial shape and amplitude periodically. Par-



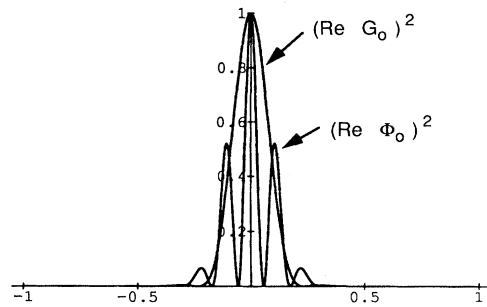
$$t = 0, \rho = 0, a_1 = 1, \beta = 3.333, \kappa = 3.333$$

FIG. 6. Comparison of Bessel-Gauss solution Φ_0 , and its envelope G_0 with $\rho=0, t=0, a_1=1 \text{ cm}, \beta=3.333 \text{ cm}^{-1}, \kappa=3.333 \text{ cm}^{-1}$.



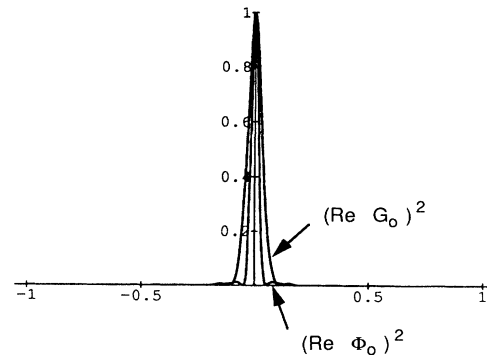
$$t = 0, \rho = 0, a_1 = 1, \beta = 3.333, \kappa = 6$$

FIG. 7. Comparison of Bessel-Gauss solution Φ_0 and its envelope G_0 with $\rho=0, t=0, a_1=1 \text{ cm}, \beta=3.333 \text{ cm}^{-1}, \kappa=6 \text{ cm}^{-1}$.



$$t = 0, \rho = 0, a_1 = 1, \beta = 33.33, \kappa = 60$$

FIG. 8. Comparison of Bessel-Gauss solution Φ_0 and its envelope G_0 with $\rho=0, t=0, a_1=1, \beta=33.33 \text{ cm}^{-1}, \kappa=60 \text{ cm}^{-1}$.



$$t = 0, \rho = 0, a_1 = 0.1, \beta = 33.33, \kappa = 60$$

FIG. 9. Comparison of Bessel-Gauss solution Φ_0 and its envelope G_0 with $\rho=0, t=0, a_1=0.1, \beta=33.33 \text{ cm}^{-1}, \kappa=60 \text{ cm}^{-1}$.

ticularly as κ/β increases and a_1 decreases, the backward traveling plane wave has little effect on the forward propagation of the pulse.

III. SUPERPOSITION USING BESSEL-GAUSS PULSES

In the bidirectional traveling-plane-wave synthesis, general solutions to the scalar wave equation can be found using Eq. (2.22) in Ref. [9],

$$\psi(\rho, \xi, \eta) = \frac{1}{(2\pi)^2} \int_0^\infty d\kappa \int_0^\infty d\alpha \int_0^\infty d\beta C_0(\alpha, \beta, \kappa) \kappa \times J_0(\kappa\rho) e^{-i\alpha\xi} \times e^{i\beta\eta} \delta\left[\alpha\beta - \frac{\kappa^2}{4}\right], \tag{13}$$

where for simplicity we have taken $n=0$ and $l=1$. This is a superposition of elementary Bessel beam solutions with an appropriate spectrum and the constraint equation included. Ziolkowski created a superposition of elementary fundamental Gaussian solutions [2,8]. This is done because these types of syntheses utilize basis functions that are localized and thus well suited to describe localized energy transmission. We have shown that Bessel-Gauss pulse solutions are even more localized than the fundamental Gaussians and are a generalization that includes both Durnin's Bessel beam solution and the fundamental Gaussian as special cases. Thus using them as basis functions in (13) should give more general localized solutions of the scalar wave equation. Then the superposition becomes

$$f(\mathbf{r}, t) = \frac{1}{(2\pi)^2} \frac{a_1}{V} \int_0^\infty d\kappa \int_0^\infty d\alpha \int_0^\infty d\beta C_0(\kappa, \beta, \alpha) \kappa \left[J_0\left[\frac{\kappa a_1 \rho}{V}\right] \exp[-\beta(\rho^2/V - i\eta) - i\alpha\xi a_1/V] \right] \delta\left[\alpha\beta - \frac{\kappa^2}{4}\right] \tag{14}$$

or performing the integration over α :

$$f(\mathbf{r}, t) = \frac{a_1}{(2\pi)^2 V} \int_0^\infty d\kappa \int_0^\infty d\beta C_0\left[\kappa, \beta, \frac{\kappa^2}{4\beta}\right] \frac{\kappa}{\beta} J_0\left[\frac{\kappa a_1 \rho}{V}\right] \exp\left[-\beta\left[\frac{\rho^2}{V} - i\eta\right] - \frac{i\kappa^2 a_1 \xi}{4\beta V}\right]. \tag{15}$$

If the spectral function $C_0(\kappa, \beta, \kappa^2/4\beta)$ satisfies certain criteria [9], then $f(\mathbf{r}, t)$ will have finite energy.

As a specific example, we use the spectrum [9]

$$C_0\left[\kappa, \beta, \frac{\kappa^2}{4\beta}\right] = (2\pi)^2 \frac{2^{-m}}{\Gamma(m)} \beta^{m-1} \exp\left[-a_2\beta - \frac{a_3\kappa^2}{4\beta}\right] \tag{16}$$

with m integer and $a_2, a_3 > 0$.

Then

$$f(\mathbf{r}, t) = \frac{2^{-m}}{\Gamma(m)} \frac{a_1}{V} \int_0^\infty d\kappa \kappa J_0(\gamma\kappa) \int_0^\infty d\beta \beta^{m-2} e^{-\beta(s+a_2)} \times e^{-\kappa^2 p/4\beta}, \tag{17}$$

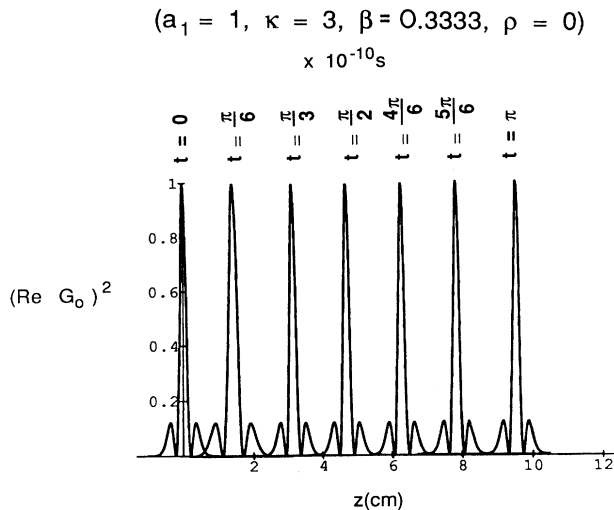


FIG. 10. Time history of the Bessel-Gauss envelope G_0 with $\rho=0$, $a_1=1$ cm, $\beta=0.3333$ cm⁻¹, and $\kappa=3$ cm⁻¹.

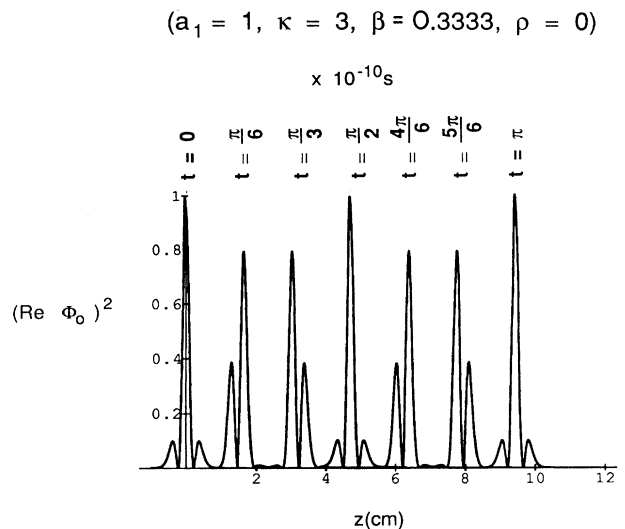


FIG. 11. Time history of the Bessel-Gauss envelope Φ_0 with $\rho=0$, $a_1=1$ cm, $\beta=0.3333$ cm⁻¹, and $\kappa=3$ cm⁻¹.

where

$$s = \frac{\rho^2}{V} - i\eta, \quad (18a)$$

$$\gamma = \frac{a_1 \rho}{V}, \quad (18b)$$

$$p = a_3 + \frac{i\xi a_1}{V}. \quad (18c)$$

Performing the integration with respect to β using Gradshteyn and Ryzhik [11], formula 3.471.9,

$$I_\beta = \int_0^\infty d\beta \beta^{m-2} e^{-\beta(s+a_2)} e^{-\kappa^2 p/4\beta} \quad (19)$$

$$= 2 \left[\frac{\kappa^2 p}{4(s+a_2)} \right]^{(m-1)/2} K_{m-1}(\kappa \sqrt{p(s+a_2)}). \quad (20)$$

Now $f(\mathbf{r}, t)$ becomes

$$f(\mathbf{r}, t) = \frac{2^{-m}}{\Gamma(m)} \frac{2a_1}{V} \left[\frac{p}{4(s+a_2)} \right]^{(m-1)/2} \times \int_0^\infty d\kappa \kappa^m J_0(\gamma\kappa) K_{m-1}(\delta\kappa), \quad (21)$$

with

$$\delta = \sqrt{p(s+a_2)}. \quad (22)$$

Finally, performing the integration over κ using Ref. [11], formula 6.576.3,

$$f(\mathbf{r}, t) = \left[\frac{a_1}{V} \right] \left[\frac{p}{4(s+a_2)} \right]^{(m-1)/2} \frac{1}{\delta^{1+m}} \times F \left[m, 1; 1; -\frac{\gamma^2}{\delta^2} \right], \quad (23)$$

where F is the hypergeometric function and can be written in the form [9,12]

$$F \left[m, 1; 1; -\frac{\gamma^2}{\delta^2} \right] = \frac{1}{\left[1 + \left(\frac{\gamma}{\delta} \right)^2 \right]^m}. \quad (24)$$

For $m=1$,

$$f(\mathbf{r}, t) = \frac{a_1}{V} \frac{1}{(\gamma^2 + \delta^2)}. \quad (25)$$

Equation (25) has the same form as the splash pulse in Ref. [2] although the variables in the denominator are different.

We can compare the splash pulse derived using a superposition of fundamental Gaussian pulses with the splash pulse derived from a superposition of Bessel-Gauss pulses. Ziolkowski's splash pulse is shown in Fig. 12 with the parameters $t=0$, $a_1=0.01$ cm, $a_2=1$ cm. The splash pulse determined with Bessel-Gauss basis functions is shown in Fig. 13 for $t=0$, $a_1=0.01$ cm, $a_2=1$ cm, and $a_3=0.01$ cm. With the extra parameter a_3 , we have achieved a sharper pulse than the splash pulse of Fig. 12. It is more highly localized near both the transverse and propagation axes. Thus with Bessel-Gauss basis func-

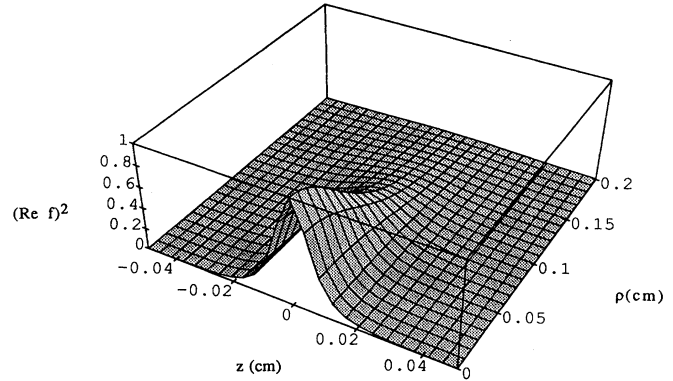


FIG. 12. Fundamental Gaussian splash pulse with $t=0$, $a_1=0.01$ cm, $a_2=1$ cm.

tions, we have created a more localized pulse than can be obtained using fundamental Gaussian basis functions.

IV. CONCLUSION

We have obtained a family of exact solutions to the scalar wave equation that describe modulated moving Bessel-Gauss pulses. The zeroth-order solution of this family was shown to include both the fundamental Gaussian solution and the Bessel beam solution (in bidirectional form) as special cases. These pulses are more localized than the fundamental Gaussians because of their extra degree of freedom over a transverse spectral parameter. Thus using them in a superposition with an appropriate spectral function produces a pulse with more highly localized propagation characteristics. We have shown only one example of such a pulse but many interesting exact solutions of the scalar wave equation may be obtained in this way.

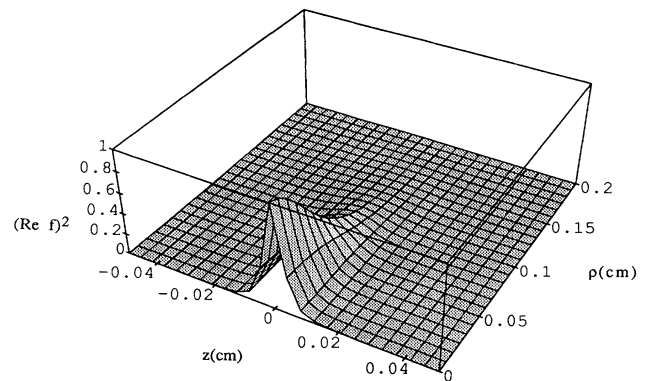


FIG. 13. Bessel-Gauss splash pulse with $t=0$, $a_1=0.01$ cm, $a_2=1$ cm, $a_3=0.01$ cm.

**APPENDIX A: DERIVATION
OF THE ZERO-ORDER BESSEL-GAUSS PULSE**

Let

$$\Phi(\mathbf{r}, t) = e^{i\beta(z+ct)} G(\rho, z-ct) \quad (\text{A1})$$

satisfy the three-dimensional scalar wave equation,

$$(\Delta - \partial_{ct}^2)\Phi(\mathbf{r}, t) = 0 \quad (\text{A2})$$

(where we assume azimuthal symmetry). Then $G(\rho, z-ct)$ satisfies

$$(\nabla_r^2 + 4i\beta\partial_\zeta)G(\rho, \zeta) = 0, \quad (\text{A3})$$

where we have transformed to $\zeta = z - ct$, $\eta = z + ct$.

Assuming the following ansatz, i.e.,

$$G(\rho, \zeta) = A_0 J_0 \left[\frac{\kappa\rho}{s(\zeta)} \right] \exp \left[iP(\zeta) + \frac{i\beta\rho^2}{q(\zeta)} \right], \quad (\text{A4})$$

where s , P , and q are functions of ζ only, Eq. (A3) yields three equations,

$$\frac{s_\zeta}{s} - \frac{1}{q} = 0, \quad (\text{A5a})$$

$$\frac{4i\beta}{q} - \frac{\kappa^2}{s^2} - 4\beta P_\zeta = 0, \quad (\text{A5b})$$

$$q_\zeta - 1 = 0. \quad (\text{A5c})$$

From (A5c),

$$q = q_0 + \zeta, \quad (\text{A6})$$

where q_0 is a constant. Then (A5a) can be solved,

$$s = s_0 q, \quad (\text{A7})$$

where s_0 is a constant also. Thus (A5b) gives

$$P = i \ln q + \frac{\kappa^2}{4\beta s_0^2 q} + P_0. \quad (\text{A8})$$

At $\zeta = 0$, we want

$$G(\rho, 0) = A_0 J_0(\kappa\rho) e^{-\beta\rho^2/a_1} \quad (\text{A9})$$

thus

$$q = \zeta - ia_1, \quad (\text{A10a})$$

$$s = \frac{iq}{a_1}, \quad (\text{A10b})$$

and

$$P = i \ln \left[1 + \left(\frac{\zeta}{a_1} \right)^2 \right]^{1/2} - \tan^{-1} \left(\frac{\zeta}{a_1} \right) - \frac{\kappa^2 a_1^2}{4\beta q} - \frac{\kappa^2 a_1}{i4\beta}. \quad (\text{A10c})$$

As in Ref. [8], by defining

$$w(\zeta) = w_0 \left[1 + \left(\frac{\zeta}{a_1} \right)^2 \right]^{1/2}, \quad (\text{A11})$$

(A4) becomes

$$G(\rho, \zeta) = A_0 J_0 \left[\frac{\kappa\rho a_1}{iq} \right] \exp \left\{ i \left[-i \ln \frac{w_0}{w(\zeta)} - \tan^{-1} \left(\frac{\zeta}{a_1} \right) - \frac{\kappa^2 a_1^2}{4\beta q} - \frac{\kappa^2 a_1}{i4\beta} \right] \right\} \exp \left[\frac{\beta\rho^2}{q} \right]. \quad (\text{A12})$$

Using

$$\frac{w_0}{w(\zeta)} e^{-i \tan^{-1}(\zeta/a_1)} = \frac{a_1}{a_1 + i\zeta}, \quad (\text{A13})$$

(A12) becomes (and setting $A_0 = 1$)

$$G(\rho, \zeta) = \frac{a_1}{(a_1 + i\zeta)} J_0 \left[\frac{\kappa\rho a_1}{a_1 + i\zeta} \right] \exp \left[-\frac{\beta\rho^2}{a_1 + i\zeta} \right] \exp \left[\frac{\kappa^2 a_1}{4\beta} \left[\frac{a_1}{a_1 + i\zeta} - 1 \right] \right] \quad (\text{A14})$$

or using $V = a_1 + i\zeta$,

$$G(\rho, \zeta) = \frac{a_1}{V} J_0 \left[\frac{\kappa\rho a_1}{V} \right] \exp \left[\frac{-\beta\rho^2}{V} \right] \times \exp \left[\frac{-i\kappa^2 a_1 \zeta}{4\beta V} \right]. \quad (\text{A15})$$

Using (A15) in (A1) gives an exact solution to the scalar wave equation,

$$\Phi_0(\mathbf{r}, t) = \frac{a_1}{V} J_0 \left[\frac{\kappa\rho a_1}{V} \right] \exp \left[-\beta \left[\frac{\rho^2}{V} - i\eta \right] - \frac{i\kappa^2 a_1 \zeta}{4\beta V} \right]. \quad (\text{A16})$$

Using the usual prescription of $\eta \rightarrow 2z$, $\zeta \rightarrow z$, $\beta \rightarrow \beta/2$, and $a_1 = \beta w_0^2$, where w_0 is the beam waist parameter at

$z=0$, (A16) reduces to a zeroth-order Bessel-Gauss beam [10].

**APPENDIX B: BIDIRECTIONAL PLANE-WAVE
DECOMPOSITION OF THE ZEROTH-ORDER
BESSEL-GAUSS SOLUTION**

The bidirectional plane-wave representation [9] in Eq. (13) can be used to derive the zeroth-order Bessel-Gauss solution in Eq. (4). We start with the spectrum

$$C_0(\alpha', \beta', \kappa') = 2\pi^2 a_1 I_0 \left[\frac{\kappa \kappa' a_1}{2\beta'} \right] \times \exp \left[-\frac{a_1(\kappa^2 + \kappa'^2)}{4\beta'} \right] \delta(\beta - \beta'), \quad (\text{B1})$$

where I_0 is a modified Bessel function of the first kind.

Substituting (B1) into Eq. (13) in the text and integrating over α' , we have

$$\Phi_0(\rho, \xi, \eta) = \frac{a_1}{2} \int_0^\infty d\kappa' \int_0^\infty d\beta' \left[\frac{\kappa'}{\beta'} \right] J_0(\kappa' \rho) I_0(\kappa' \sigma_1) e^{-a_1(\kappa^2 + \kappa'^2)/4\beta'} e^{-i\kappa^2 \xi / 4\beta'} e^{i\beta' \eta} \delta(\beta - \beta'), \quad (\text{B2})$$

with

$$\sigma_1 = \frac{\kappa a_1}{2\beta'}. \quad (\text{B3})$$

The κ' integration can be written

$$L_{\kappa'} = \int_0^\infty d\kappa' \kappa' J_0(\kappa' \rho) I_0(\kappa' \sigma_1) e^{-\kappa'^2 V / 4\beta'} \quad (\text{B4})$$

$$= \frac{2\beta'}{V} \exp \left[\frac{(\sigma_1^2 - \rho^2)\beta'}{V} \right] J_0 \left[\frac{2\sigma_1 \rho \beta'}{V} \right] \quad (\text{B5})$$

using formula 6.633.4 in Ref. [11]. The β' integration is now

$$\Phi_0(\rho, \xi, \eta) = a_1 \int_0^\infty d\beta' \delta(\beta - \beta') e^{-a_1 \kappa^2 / 4\beta'} e^{i\beta' \eta} \times \left[\frac{1}{V} \exp \left[\frac{(\sigma_1^2 - \rho^2)\beta'}{V} \right] \times J_0 \left[\frac{2\sigma_1 \rho \beta'}{V} \right] \right]. \quad (\text{B6})$$

Due to the Dirac δ function, (B6) is simply

$$\Phi_0(\rho, \xi, \eta) = \frac{a_1}{V} J_0 \left[\frac{2\sigma_1 \rho \beta}{V} \right] \times \exp \left[\frac{-\beta \rho^2}{V} + \frac{\sigma_1^2 \beta}{V} - \frac{a_1 \kappa^2}{4\beta} + i\beta \eta \right] \quad (\text{B7})$$

or

$$\Phi_0(\rho, \xi, \eta) = \frac{a_1}{V} J_0 \left[\frac{\kappa a_1 \rho}{V} \right] \exp \left[-\beta \left[\frac{\rho^2}{V} - i\eta \right] - \frac{\kappa^2 a_1}{4\beta} \right] \times \left[1 - \frac{a_1}{V} \right] \quad (\text{B8})$$

or finally

$$\Phi_0(\rho, \xi, \eta) = \frac{a_1}{V} J_0 \left[\frac{\kappa a_1 \rho}{V} \right] \times \exp \left[-\beta \left[\frac{\rho^2}{V} - i\eta \right] - \frac{i\kappa^2 a_1 \xi}{4\beta V} \right], \quad (\text{B9})$$

which is the same as Eq. (4).

- [1] J. N. Brittingham, *J. Appl. Phys.* **54**, 1179 (1983).
 [2] R. W. Ziolkowski, *J. Math. Phys.* **26**, 861 (1985).
 [3] P. A. Belanger, *J. Opt. Soc. Am. A* **1**, 723 (1984).
 [4] A. Sezginer, *J. Appl. Phys.* **57**, 678 (1985).
 [5] P. Hillion, *Wave Motion* **10**, 143 (1988).
 [6] J. Durnin, *J. Opt. Soc. Am. A* **4**, 651 (1987).
 [7] J. Durnin, J. J. Miceli, and J. H. Eberly, *Phys. Rev. Lett.* **58**, 1499 (1987).
 [8] R. W. Ziolkowski, *Phys. Rev. A* **39**, 2005 (1989).

- [9] I. M. Besieris, A. M. Shaarawi, and R. W. Ziolkowski, *J. Math. Phys.* **30**, 1254 (1989).
 [10] F. Gori, G. Guattari, and C. Padovanni, *Opt. Comm.* **64**, 491 (1987).
 [11] I. S. Gradshteyn and I. M. Ryzhik, *Tables of Integrals, Series, and Products* (Academic, New York, 1976).
 [12] *Handbook of Mathematical Functions*, Natl. Bur. Stand. Appl. Math. Ser. No. 55, edited by M. Abramowitz and I. Stegun (U.S. GPO, Washington, DC, 1964).